HHS Public Access

Author manuscript

Cell. Author manuscript; available in PMC 2017 May 19.

Published in final edited form as:

Cell. 2016 May 19; 165(5): 1160–1170. doi:10.1016/j.cell.2016.04.016.

The cell nucleus serves as a mechanotransducer of tissue damage-induced inflammation

Balázs Enyedi, **Mark Jelcic**, and **Philipp Niethammer***

Cell Biology Program, Memorial Sloan Kettering Cancer Center, New York, NY 10065, USA

SUMMARY

Tissue damage activates cytosolic phospholipase A_2 ($cPLA_2$), releasing arachidonic acid (AA), which is oxidized to proinflammatory eicosanoids by 5-lipoxygenase (5-LOX) on the nuclear envelope. How tissue damage is sensed to activate $cPLA_2$ is unknown. We investigated this by live imaging in wounded zebrafish larvae, where damage of the fin tissue causes osmotic cell swelling at the wound margin and the generation of a chemotactic eicosanoid signal. Osmotic swelling of cells and their nuclei activates $cPla_2$ by translocating it from the nucleoplasm to the nuclear envelope. Elevated cytosolic Ca^{2+} was necessary but not sufficient for $cPla_2$ translocation, and nuclear swelling was required in parallel. $cPla_2$ translocation upon nuclear swelling was reconstituted in isolated nuclei, and appears to be a simple physical process mediated by tension in the nuclear envelope. Our data suggest that the nucleus plays a mechanosensory role in inflammation, by transducing cell swelling and lysis into proinflammatory eicosanoid signaling.

INTRODUCTION

Swelling is a common cellular stress-state that precedes necrotic cell death (Berghe et al., 2014; Majno and Joris, 1995). Histologically termed ‘cytotoxic edema’ (Liang et al., 2007), pathological cell swelling results from severe tissue stress, for instance, caused by ischemia or blunt trauma. In ischemia, cell swelling is associated with elevated levels of free fatty acids (incl. AA and its metabolites) (Bazán, 1970) and “sterile” leukocyte recruitment that can impede tissue repair. Cell swelling and release of AA-derivatives also characterize a highly inflammatory form of macrophage necrosis, termed pyroptosis (Berghe et al., 2014; von Moltke et al., 2012). The lead hypothesis to explain leukocyte recruitment in these instances is that cell swelling triggers cell lysis, which releases proinflammatory cytoplasmic factors into the extracellular space (Rock et al., 2011). However, recent studies showed that cell swelling directly activates inflammatory cascades independent of cell lysis

*Correspondence to: Philipp Niethammer (; Email: niethamp@mskcc.org).

SUPPLEMENTAL INFORMATION includes Extended Experimental Procedures, six supplemental figures and eight movies.

AUTHOR CONTRIBUTIONS

P.N. and B.E. conceived the project and designed the experiments. B.E., P.N., and M.J. performed the experiments. B.E. developed computational tools and wrote computer code to analyze the data. P.N. and B.E. wrote the paper.

(Compan et al., 2012; Enyedi et al., 2013). The mechanisms that underlie cell swelling-induced inflammation remain poorly understood.

Zebrafish are a powerful system to study conserved, inflammatory mechanisms in a live vertebrate (LeBert and Huttenlocher, 2014). Analogous to the epithelial linings of the upper digestive tract of mammals, the epithelia of zebrafish larvae are exposed to a hypotonic external environment. Epithelial wounds expose internal tissues to hypotonicity, which leads to osmotic cell swelling. This triggers translocation of $cPla_2$ from its resting localization in the nucleoplasm to the inner nuclear membrane (INM) in cells at injury sites. $cPLA_2$ sets the rate limiting step for AA release from the sn-2 position of membrane phospholipids. AA is metabolized by nuclear 5-lipoxygenase into chemotactic eicosanoids that attract leukocytes to the epithelial breach (Enyedi et al., 2013). It is unclear why the chemoattractive $cPLA_2$-5-LOX arm of AA-metabolism uses the nuclear envelope as an activation scaffold (Brock, 2005). In contrast to the plasma membrane, the membranes of the nuclear envelope rarely undergo surface area fluctuations and are supported by a shock-absorbing lamina (Dahl et al., 2004, 2008). Their intrinsic quiescence and stability should make them uniquely suited to selectively respond to severe, extrinsic perturbations, such as cell swelling (Enyedi and Niethammer, 2016). We speculated that illuminating the mechanism of $cPLA_2$ activation by cell swelling could shed light on novel nuclear functions.

RESULTS

Hypotonic Exposure and Ca^{2+} are required for $cPla_2$ Activation in Zebrafish

Intracellular Ca^{2+} is the main known activator of $cPLA_2$ (Burke and Dennis, 2009). To test whether cell swelling induces Ca^{2+} signals *in vivo*, and whether these signals are sufficient for osmotic $cPLA_2$ activation, we imaged the spatiotemporal patterns of nuclear [Ca^{2+}] and INM-translocation of $cPla_2$ after zebrafish tail fin wounding (Figure 1A, B). Using a nuclear targeted, genetically encoded Ca^{2+}-reporter (GCaMP6s) (Chen et al., 2013), we identified three types of Ca^{2+} transients triggered by tail fin wounding: A fast inwards-moving (~ 5 μm/sec) wave, a persistent wound margin signal, and an oscillatory activity that extended ~ 200 μm deep into the fish and lasted for ~3 min (Figure 1B, S1A, Movie S1). Increasing the osmolarity of the bathing solution blocks cell swelling at the wound margin and the generation of leukocyte chemoattractants (Enyedi et al., 2013; Gault et al., 2014). The fast Ca^{2+} wave was slightly, and the wound margin signal moderately affected by increasing the osmolarity of the bathing medium (Figure 1B, S1A, Movie S1). In contrast, the oscillatory activity was blocked by immersing fish in isotonic medium, showing its dependence on osmotic cell swelling (Figure 1C, S1A). We followed $cPLA_2$ activation by imaging zebrafish $cPla_2$ fused to an mKate2 fluorophore ($cPla_2$-mK2) as previously described (Enyedi et al., 2013). If swelling-induced Ca^{2+} signals were sufficient for osmotic $cPLA_2$ activation, we would expect $cPla_2$-mK2 INM-translocation to be spatially correlated with the oscillatory Ca^{2+} activity. This was not strictly the case: $cPla_2$-mK2 INM-translocation overlapped with Ca^{2+} signals close to the wound margin, but not at a greater distance (Figure 1D, E, S1B).

Ionophore-induced Ca^{2+} levels were insufficient to translocate $cPla_2$-mK2 without osmotic stimulation, that is, in isotonic bathing solution (Figure S2). By contrast, combined ionophore and hypotonic stimulation led to a slow-moving Ca^{2+} wave-front that was closely

correlated with $cPla_2$ INM-translocation in wounded tail fins (Figure S2B–E, Movies S2 and S3). Fibroblast-like cells with dendritic nuclei (Mateus et al., 2012), showed a particular propensity for $cPla_2$-mK2 translocation (Figure S2E–G). These data suggest that osmotic cell swelling contributes an essential, second signal that governs Ca^{2+}-dependent $cPla_2$ activation through INM-recruitment of the enzyme.

Reconstituting Cell Swelling-Induced $cPla_2$ Activation in HeLa Cells

To determine the minimal requirements for cell swelling-induced $cPLA_2$ activation, we reconstituted this mechanism by heterologous expression of $cPla_2$-mK2 in HeLa cells. As in zebrafish larvae, $cPla_2$-mK2 was predominantly located in the nucleoplasm of HeLa cells before activation (Figure 2A). Hypotonic shock triggered rapid INM-association of $cPla_2$ (Enyedi et al., 2013), and consistent with previous cell culture data (Thoroed et al., 1997), also increased [^{3}H] AA release (Figure 2B, C). In rare cases (<2% of cells), $cPla_2$-mK2 was localized in the cytoplasm under resting conditions, and translocated to the ER and outer nuclear membrane upon activation (Figure S3A). Membrane association of $cPla_2$ thus does not require nuclear proteins such as nuclear lamins. The cell culture model allowed us to correlate [Ca^{2+}] and $cPla_2$-mK2 translocation on a cell-by-cell basis. Ca^{2+} signals were induced either by hypotonic shock or purinergic receptor stimulation with ATP. As expected for a Ca^{2+} dependent enzyme, $cPla_2$ translocation never occurred below a critical Ca^{2+} threshold (Figure 2D). Corroborating our *in vivo* data, suprathreshold Ca^{2+} signals induced by hypotonic shock were ~2.5 times more efficient in translocating $cPla_2$-mK2 in HeLa cells than purinergic Ca^{2+} signals of the same amplitude, but without osmotic stimulation (Figure 2D).

$cPLA_2$ is regulated by kinases that phosphorylate the enzyme itself or generate phospholipids that bind to the enzyme (for example, ceramide-1-phosphate) (Burke and Dennis, 2009). However, osmotic $cPla_2$-mK2 translocation efficiency was not decreased by pan-kinase inhibition (staurosporine), mutation of $cPla_2$'s conserved Ser498 (=Ser505 of human $cPLA_2$) phosphorylation site into alanine or glutamate, or specific pharmacological inhibition of ceramide kinase with NVP231 (Figure S3B) (Graf et al., 2008). Thus, osmotic cell swelling appears to trigger translocation and activation of $cPla_2$ through a new mechanism that operates dependent on Ca^{2+} signals, but independent of other known regulators.

F-actin and the Nuclear Lamina Regulate Swelling-induced $cPLA_2$ Activation

Hypotonic shock leads to water influx and swelling of the nucleus along with the cytoplasm (Dahl et al., 2004; Finan and Guilak, 2010). F-actin filaments and the nuclear lamina control nuclear morphology in intact cells (Khatau et al., 2009; Rowat et al., 2008). Actin depolymerization by latrunculin A or B (LA/LB) approximately doubled the relative nuclear volume increase after hypotonic shock both in HeLa cells and in the epithelial cells of live zebrafish (Figure 2E, 3E). At the same time, actin depolymerization increased the ability of Ca^{2+} signals to trigger $cPla_2$-mK2 translocation in HeLa cells and live zebrafish larvae (Figure 2D, 3A–D, and Movie S4). LB pretreatment enabled Ca^{2+} oscillations to translocate $cPla_2$-mK2 to the INM at a distance > 100 μm away from the wound margin (Figure 3C, D), where translocation was never observed without LB (Figure 1D, E). Thus, the actin

cytoskeleton tunes the osmotic activation threshold in isolated cells and intact tissues, possibly by modulating the dynamics of nuclear swelling. Although our experiments do not exclude a potential role for nuclear actin, cytoplasmic F-actin structures, such as the "perinuclear actin cap," are principally well-positioned to restrain volume expansion of the nucleus (Khatau et al., 2009). Furthermore, cytoplasmic F-actin is mechanically coupled to the nuclear lamina through LINC complexes (Starr and Fridolfsson, 2010). Force transmission via this linkage has been shown to stiffen the lamina (Guilluy et al., 2014), so severing nucleocytoplasmic coupling by LA/LB may soften it. The observed 20–40% volume increase of osmotically challenged nuclei cannot be exclusively explained by the 2–4% area expansion (corresponding to ~3–6% volume expansion of spherical nuclei) that lipid bilayers can undergo without rupturing (Hamill and Martinac, 2001). F-actin may negatively regulate nuclear surface reservoirs, in addition to potential mechanical stabilization functions.

The nuclear lamina becomes softer by lamin A/C (LMNA) depletion (Lammerding et al., 2004; Swift et al., 2013). We hypothesized that a softer lamina would be less able to dissipate mechanical force acting on the nuclear envelope, leading to an increase of nuclear membrane tension. RNAi-mediated LMNA depletion of HeLa cells led to an increase in $cPla_2$ translocation upon osmotic stimulation (Figure 4A, B). Unlike LA treatment, LMNA depletion did not further enhance nuclear volume expansion (Figure 4C). These data are consistent with the idea that nuclear membrane tension is increased by LMNA depletion to promote $cPla_2$-INM interactions. The signaling consequences of LMNA depletion could be more complex. Our experiments clearly argue against a requirement of lamin A/C for swelling-induced $cPla_2$ translocation to the INM, but do not rule out other regulatory functions of lamin A/C aside from modulatory effects on nuclear membrane tension. Altogether, the data agree that $cPla_2$-INM interactions critically depend on the mechanical and structural properties of the nucleus.

Nuclear Swelling Promotes the Accumulation of $cPla_2$ and 5-LOX on the INM

To test whether nuclear swelling directly causes $cPla_2$ activation, we further simplified our experimental system by permeabilizing HeLa cells with low concentrations of digitonin. This compound binds cholesterol to specifically perforate plasma but not nuclear membranes. Nucleoplasmic $cPla_2$-mK2 fluorescence was retained in most cells during digitonin-treatment, confirming that the nuclear membranes remained intact. Leakage of cytoplasmic macromolecules after lysis reduces the extranuclear oncotic pressure, which leads to nuclear swelling. To counteract the loss of extranuclear oncotic pressure and prevent nuclear swelling upon lysis, we permeabilized cells in the presence of 360 kDa polyvinylpyrrolidone (PVP), a synthetic polymer too large to pass through nuclear pores. In this experiment, $[Ca^{2+}]$ is precisely adjustable, and nuclear swelling can be induced by dilution of PVP. Under these circumstances, both Ca^{2+} and nuclear swelling controlled the translocation of $cPla_2$ to the INM. Swelling augmented membrane accumulation of the enzyme at low-to-intermediate $[Ca^{2+}]$ (300 nM – 1400 nM), namely, levels consistent with signal- as opposed to damage-induced Ca^{2+} (Figure 5A, B, Figure S4A and Movie S5). We also observed swelling-mediated INM accumulation with a truncated construct comprising the C2-domain of $cPla_2$ (Figure 5B), and with fish or human full-length 5-LOX (Figure

S4B). The C2 domains of 5-LOX and $cPLA_2$ are highly related and required for membrane binding and activity of these enzymes.

We reconstituted swelling-induced C2-domain binding to lipid bilayers on giant vesicles (GVs) *in vitro*. GVs are a heterogeneous mixture of more or less multilayered ("onion-like") vesicles of various sizes prepared by exposing a dried lipid film to water (Needham et al., 1988). Depending on their particular membrane stratification and solvent content, GVs display varying propensity for swelling upon exposure to hypotonic solution. GVs were prepared to contain PBS + 300 mM Sucrose. Upon exposure to hypotonic solution (PBS alone) complemented with Ca^{2+} and recombinant $cPla_2$-C2 domain tagged with EGFP, a subfraction of GVs showed morphological signs of swelling, such as a mild increase of circularity, and cross sectional area. The moderate volume increases of GVs suggest that these vesicles, unlike nuclei, do not possess large, accessible surface reservoirs. A sudden change toward a more irregular vesicle morphology allowed us to discern the moment of osmotically-induced rupture that ended the swelling (Figure 5C, Movie S6). Before vesicle bursting, the fluorescent C2 domain rapidly accumulated on the membrane of swelling GVs, and vesicle rupture, which releases membrane tension, was accompanied by a loss of C2 domain from the membrane. By contrast, GVs exposed to isotonic solution (PBS+300 mM Sucrose), never showed signs of swelling or rupture, nor the characteristic rapid accumulation of $cPla_2$-C2-EGFP on the rim (Figure 5C, Movie S6). These experiments indicate that GV swelling enhances membrane association of $cPla_2$'s C2 domain, and/or decreases its dissociation. They show that the C2 domain of $cPla_2$, in the presence of Ca^{2+}, is a direct sensor of membrane tension, and that accessory proteins are not necessary for this intrinsic function.

Consistent with this notion, cell permeabilization, which produces high [Ca^{2+}] and nuclear swelling, triggered INM-translocation of $cPla_2$-mK2 (Figure S5) in zebrafish larvae regardless of bathing osmolarity. By contrast, ionomycin, which produces high intracellular [Ca^{2+}] but no nuclear swelling, only translocated $cPla_2$-mK2 together with hypotonic cell swelling as shown above (Figure S2D, F). Together, these observations underline the necessity of nuclear swelling, either induced by cell lysis or osmotic cell swelling, as a physiological costimulus for $cPla_2$ activation.

Mechanical Compression of the Nucleus Triggers $cPla_2$ Activation

Besides osmotic swelling, stretching the nucleus by simple mechanical compression was enough to promote $cPla_2$ accumulation on the INM at suprathreshold [Ca^{2+}] (Figure 5D, Movie S7). Swelling- and compression-induced INM-recruitment of $cPla_2$ occurred in the absence of ATP or other cytoplasmic components under permeabilized conditions, indicating that kinase signaling was not required. Diffusion of nucleoplasmic $cPla_2$-EGFP (~6.6 μm^2/sec), as measured by fluorescence recovery after photobleaching, was on the order of magnitude expected for a freely diffusible cytoplasmic protein of that size (Figure S6) (Kang et al., 2012). Ca^{2+} stimulation strongly decreased $cPla_2$-EGFP diffusion (~0.05 μm^2/sec) to a range consistent with a membrane-bound protein (Figure S6) (Hammond et al., 2009). Diffusion was not affected by nuclear swelling (Figure S6), arguing against the possibility that macromolecular crowding in the nucleus, which should decrease with nuclear swelling,

inhibits $cPla_2$ by hindering enzyme diffusion to the INM. Collectively, our data indicate that nuclear swelling and compression mechanically enhance the INM-$cPla_2$ interactions. They are consistent with the long-standing notion that various membrane enzymes, including certain soluble PLA_2 isoforms, are sensitive to changes in lateral bilayer pressure, for instance, induced by osmotic swelling of liposomes *in vitro* (Boguslavsky et al., 1994; Lehtonen and Kinnunen, 1995; Slater et al., 1994). However, until now, *in vivo* evidence establishing a physiological context for this mechanotransduction paradigm has been lacking.

Swelling Decreases $cPla_2$ Dissociation from the Nuclear Envelope

To further test how nuclear swelling affects INM-$cPla_2$ interactions, we stimulated membrane binding in permeabilized cells by high Ca^{2+} (Figure 5E). Ca^{2+} was then washed out, and we measured $cPla_2$-mK2 dissociation from swollen and nonswollen nuclei using confocal fluorescence microscopy. Without Ca^{2+}, $cPLA_2$ cannot bind the membrane, so only membrane dissociation of the enzyme is observed. Membrane dissociation followed exponential, first-order decay kinetics, and occurred much faster on nonswollen than on swollen nuclei as indicated by a ~2-fold difference in apparent k_{off} (Figure 5E, Movie S8). This suggests that $cPla_2$ membrane complexes of different strength exist, with more stable $cPla_2$-INM interactions preferentially occurring on swollen nuclei. Likely, the stability of membrane complexes is governed by the extent of hydrophobic interactions between the membrane and the enzyme. We propose that nuclear swelling activates $cPLA_2$ through enhancing its hydrophobic membrane insertion, which is crucial for its catalytic activity (Lichtenbergova et al., 1998).

Necrotic Cell Corpses Require Nuclear Swelling and $cPla_2$ to Attract Leukocytes

Our data have revealed a simple, biophysical mechanism for leukocyte recruitment to swollen cells that explains how zebrafish tissues can transduce homeostatic information on barrier damage (namely, a drop of interstitial osmotic pressure) into rapid inflammatory signaling. Since cell swelling is a hallmark of many pathological tissue perturbations, and as eicosanoid pathway enzymes are widely expressed (see Human Protein Atlas) (Uhlén et al., 2005), this mechanism may broadly contribute to inflammatory events in mammals.

Our experiments raised the possibility that necrotic cell corpses may attract leukocytes by the same mechanism as intact, swelling cells, given that their nuclei are intact. To test this, we exposed amputated tail fin tips bathed in isotonic solution to experimentally conditioned suspensions of our above characterized cell system. As predicted, cell corpses recruited leukocytes, and this required nuclear swelling and $cPla_2$, whereas strong Ca^{2+} signals alone were insufficient to exert this effect (Figure 6). By preventing loss of $cPla_2$ after cell lysis, the nucleoplasmic localization of this enzyme appears to turn the nucleus into a “panic room” for necrotactic signaling. The mechanisms of nuclear targeting of $cPLA_2$, 5-LOX, and possibly other inflammatory membrane enzymes are therefore of medical interest.

DISCUSSION

Cell swelling, cell lysis, and eicosanoid signaling are widely involved in inflammatory pathology. Our experiments reveal that cell swelling and lysis (Figure 7) are sensed through nuclear swelling, and that $cPLA_2$ and 5-LOX transduce membrane stretch caused by nuclear swelling into inflammatory eicosanoid signaling. We propose that the nucleus plays a general mechanosensory role in inflammation, explaining why $cPLA_2$ and 5-LOX localize to nuclei in many tissues (Brock, 2005). According to this idea, not only what leaks out of lysing cells (namely, cytoplasmic DAMPs) could be inflammatory, but also the cell corpses that are left behind. These corpses may signal from beyond their grave through their swollen organelles. Whether organelle swelling, before or after cell lysis, constitutes a more general, sterile inflammatory trigger akin to cytoplasmic leakage is to be seen.

Our study has interesting cell biological implications. The lamina is widely regarded as the primary mechanosensitive structure of the nucleus. Here, we show that nuclear membrane stretch directly activates $cPLA_2$ and 5-LOX, probably through enhancing enzyme insertion into the lipid bilayer. Although our results indicate that lipid bilayer stretch together with Ca^{2+} is sufficient to account for swelling-induced $cPla_2$ activation, they do not exclude potential modulatory contributions of other accessory proteins and mechanisms *in vivo*. For example, by supporting the INM, the nuclear lamina may modulate the force acting on nuclear membranes, or exert other regulatory roles. The LINC complex attaches the nuclear lamina to actin filaments, which are linked to the extracellular matrix through focal adhesions (Lombardi et al., 2011). Our study raises the question of whether and how nucleocytoplasmic coupling of cells to their extracellular environment regulates inflammatory lipid signaling.

Besides being the precursor of many inflammatory lipids, the $cPLA_2$ product AA is also required for the synthesis of certain ion channel modulators. For example, sensing hypotonic stress by the TRPV4 channel is mediated by 5,6-epoxyeicosatrienoic acid, which is generated from AA by cytochrome P450 epoxygenase (Vriens et al., 2004; Watanabe et al., 2003). Is it possible that this well-known, swell-sensing plasma membrane channel detects nuclear instead of plasma membrane stretch?

Nuclear membrane tension probably occurs in many pathophysiological situations. Cell spreading has been reported to activate an unknown stretch-sensitive Ca^{2+} channel on the outer nuclear membrane, implying that cell spreading can cause nuclear membrane stretch (Itano et al., 2003). Rupture of nuclei in rapidly proliferating cancer cells or in cells of patients with laminopathy (Davidson and Lammerding, 2014; Vargas et al.; De Vos et al., 2011) implies a preceding increase of nuclear membrane tension. Aside from hypotonic, ischemic, or necrotic cell swelling (see introduction), leukocyte extravasation and rapid migration through confined tissue channels may put nuclear membranes under stress (Friedl et al., 2011). In all these cases, the possible signaling consequences of increased nuclear membrane tension warrant attention.

EXPERIMENTAL PROCEDURES

Plasmid construction

Plasmids were created by standard molecular biology procedures as detailed in the Extended Experimental Procedures.

Zebrafish Procedures and Generation of Transgenic Lines

Casper background (White et al., 2008), wild type, and transgenic zebrafish strains were maintained as described (Nüsslein-Volhard and Dahm, 2002) with the approval of the Institutional Animal Care and Use Committee (IACUC). Zebrafish larvae were raised in E3 medium (5 mM NaCl, 0.17 mM KCl, 0.33 mM $CaCl_2$, 0.33 mM $MgSO_4$). For wounding assays, 2.5–3 day post fertilization (dpf) larvae were anesthetized using 0.2 mg/ml tricaine (Sigma) in E3 for at least 20 min before, and during laser wounding and imaging.

To generate transgenic lines, a solution containing 25–25 pg of the hsp70l:GCaMP6s-NLS-P2A-mK2-NLS, lysC:PM-mK2 or hsp70l:$cPla_2$-mK2 plasmid and transposase mRNA was injected into the cytosol of one-cell stage casper embryos. Injected larvae with mosaic cardiac EGFP expression were raised to sexual maturity and screened by crossing with wild-type fish to identify founders. F1 embryos were identified by cardiac EGFP expression and raised to sexual maturity. Experiments were performed on the progeny of F1 outcross with wild-type fish.

Maintaining and generating wild type, stable, knockdown and knockout cell lines

HeLa (CCL-2) cells were obtained from American Type Culture Collection (Manassas, VA) and maintained in DMEM supplemented with 10% fetal calf serum, 50 units/ml penicillin, and 50 μg/ml streptomycin in a 5% humidified CO_2 incubator at 37 °C. Cells were transfected with Lipofectamine 3000, Lipofectamine RNAiMAX (Invitrogen) or electroporated with the Neon® Transfection System (Invitrogen), following the manufacturer's instructions.

For establishing stable HeLa cell lines expressing $cPla_2$-mK2, $cPla_2$-EGFP, $cPla_2$-C2-mK2 or the mK2-5-LOX constructs from the pSB/CMV/MCS/Puro plasmid, cells were cotransfected in 1:10 ratio with the SB100x *Sleeping Beauty* transposase and the vectors encoding the reporters (Izsvák et al., 2009). After growing the cells in the presence of 2 μg/ml puromycin for one week, mKate2 (mK2) positive cells were isolated by flow cytometry on a BD Aria FACS, using 561 nm excitation and 670/30 nm emission wavelengths.

To silence Lamins A/C expression the following siRNAs were used at a concentration of 40 nM: si1-LMNA- CCAGGAGCTTCTGGACATCAA (SI02662597, Qiagen) and si2-LMNA-GGTGGTGACGATCTGGGCT (D-001050-01-05, Dharmacon). As a negative control, the ON-TARGETplus Non-targeting Pool siRNA mix was used (D-001810-10, Dharmacon).

To knock out endogenous $cPLA_2$ from HeLa cells, the CRISPR-Cas9 system was used by transiently expressing Cas9 fused through a 2A self-cleaving peptide to GFP from the plasmid pSpCas9(BB)-2A-GFP:$cPLA_2$-g1. Two days after transfection, flow cytometry was

used to isolate the population that showed strong GFP expression. Single cell colonies were then grown, and individually screened for $cPLA_2$ expression by immunoblotting.

Microscopy

Spinning disk confocal and widefield fluorescence microscopy was performed as detailed in the Extended Experimental Procedures.

Image Processing and Analysis

All image processing tasks were performed with the open-source program Fiji and the Anaconda distribution of the Python programming language, using custom scripts, as detailed in the Extended Experimental Procedures.

[^{3}H] Arachidonic Acid Release and Immunoblot Analysis

[^{3}H] arachidonic acid (AA) release by HeLa cells was measured according to previously established protocols (Briand et al., 1998). Cells seeded on 12 well plates at a density of $5x10^4$ cells/well were loaded with 0.1 μCi/ml [^{3}H] AA (PerkinElmer) for 20h in DMEM containing 0.1% fatty acid-free BSA (Sigma). The cells were then washed three times with EC medium containing 0.5% BSA, and stimulated for 10 min at room temperature with 800 μl control or hypotonic (150 mOSM) EC medium containing 0.5% BSA. The supernatant was then immediately removed for counting in a BD scintillation counter, and 400 μl of 0.1 N NaOH was added to lyse the cells to measure total incorporation of [^{3}H] AA. Standard immunoblot analysis was performed using antibodies against $cPLA_2$ (Abcam 135825), Lamin A/C (Cell Signaling #2032), actin (Sigma A5316) and GAPDH (Cell Signaling #2118).

Expression and Purification of Recombinant $cPla_2$-C2-EGFP-6HIS

Expression of the C2-domain of zebrafish $cPla_2$ C-terminally tagged with EGFP was induced by 0.5 mM IPTG (Promega) in a 250 ml culture of *Escherichia coli* BL21 (OD_{600} = 0.5) under vigorous shaking for ~7 h at room temperature. Cells were pelleted at 4000xg and frozen at −80 °C. Purification was performed using the QIAexpress Ni-NTA Fast Start Kit (QIAGEN) according to the manufacturer's protocol. Buffer exchange into PBS (Sigma) was performed by repeated dilution/centrifugation of the Ni-NTA eluate using a Microsep device (Pall Corporation). Protein concentration was calculated from A280 absorption on a NanoVue spectrophotometer (GE Healthcare) using the theoretical molar extinction coefficient of the protein (Protean, DNASTAR Lasergene 8). Aliquots were snap-frozen on liquid nitrogen and stored at −80 °C.

Preparation of Giant Vesicles (GVs) and Swelling Experiments

GVs were principally prepared as previously described (Needham et al., 1988). Briefly, 40 μl of a lipid mixture containing 11.25 mg/ml 1,2-dipalmitoyl-*sn*-glycero-3-phosphocholine (Avanti Polar Lipids) and 1 mg/ml 1,2-Diacyl-sn-glycero-3-phospho-L-serine (bovine brain, Sigma) in 2:1 chloroform/methanol solvent was distributed on a clean, roughened Teflon disk of 3.5 cm diameter. The lipid film was dried ~6 h under vacuum in a desiccator. The disk was tightly fitted in a glass beaker, and the lipid film was moistened with a warm, water

saturated N_2 stream. 10 ml warm, sterile filtered PBS + 300 mM Sucrose (MP Biomedicals) was added onto the disk. The beaker was sealed with Parafilm and placed at 42 °C overnight for vesicle budding. The vesicle suspension was diluted with 4 volumes of PBS + 150 mM NaCl and GVs were pelleted at 1000xg and resuspended in PBS + 300 mM Sucrose. 5–10 µl drops of the concentrated vesicle suspension were placed onto polylysine coated glass bottom dish, and left several hours at room temperature for vesicle sedimentation. The swelling experiment was started by replacing the liquid on top of the sedimented vesicles with PBS (hypotonic) or PBS + 300 mM Sucrose (isotonic) supplemented with 9.3 µM $cPla_2$-C2-EGFP and 0.5 mM $CaCl_2$ (Sigma). Time-lapse DIC and EGFP-emission images of GVs immersed in hypo- or isotonic solution were simultaneously acquired on a Nikon Eclipse Ti inverted microscope, using a 20x Plan Apochromat NA 0.75 air objective lens (Nikon) and an Andor Clara CCD camera. Green fluorescence was excited with a LED light source (Lumencor) using the bandpass 475/28 filter, a 470/40 excitation filter in conjunction with a multispectral dichroic (Chroma, 59022 bs) and emission was collected using the 525/50 emission filter set (Chroma).

Statistics

All error bars indicate standard errors of means (SEM). All p-values have been derived by an unpaired, two-tailed t-test assuming unequal variances (heteroscedastic) using Excel (Microsoft).

Supplementary Material

Refer to Web version on PubMed Central for supplementary material.

Acknowledgments

The authors would like to thank Tim Mitchison and Michelina Stoddard for their thoughtful comments on the manuscript, and Kris Noel Dahl, Alan Hall (1952–2015), Péter Enyedi and András Kapus for helpful discussions along the way. We thank Emily Foley for granting access to her confocal microscope. B.E. was supported by a Lucille Castori Center for Microbes, Inflammation and Cancer Fellowship. Research was funded by the National Institutes of Health grant GM099970, American Asthma Foundation Scholar grant, and a Louis V. Gerstner, Jr. Young Investigator award to P.N., and in part through the NIH/NCI Cancer Center Support Grant P30CA008748.

References

Bazán NG. Effects of ischemia and electroconvulsive shock on free fatty acid pool in the brain. Biochim Biophys Acta. 1970; 218:1–10. [PubMed: 5473492]

Berghe T, Vanden Linkermann A, Jouan-Lanhouet S, Walczak H, Vandenabeele P. Regulated necrosis: the expanding network of non-apoptotic cell death pathways. Nat Rev Mol Cell Biol. 2014; 15:135–147. [PubMed: 24452471]

Boguslavsky V, Rebecchi M, Morris AJ, Jhon DY, Rhee SG, McLaughlin S. Effect of monolayer surface pressure on the activities of phosphoinositide-specific phospholipase C-beta 1, -gamma 1, and -delta 1. Biochemistry. 1994; 33:3032–3037. [PubMed: 8130216]

Briand SI, Bernier SG, Guillemette G. Monitoring of phospholipase A2 activation in cultured cells using tritiated arachidonic acid. Methods Mol Biol. 1998; 105:161–166. [PubMed: 10427559]

Brock TG. Regulating leukotriene synthesis: the role of nuclear 5-lipoxygenase. J Cell Biochem. 2005; 96:1203–1211. [PubMed: 16215982]

Burke JE, Dennis Ea. Phospholipase A2 structure/function, mechanism, and signaling. J Lipid Res. 2009; 50(Suppl):S237–S242. [PubMed: 19011112]

Chen TW, Wardill TJ, Sun Y, Pulver SR, Renninger SL, Baohan A, Schreiter ER, Kerr Ra, Orger MB, Jayaraman V, et al. Ultrasensitive fluorescent proteins for imaging neuronal activity. Nature. 2013; 499:295–300. [PubMed: 23868258]

Compan V, Baroja-Mazo A, López-Castejón G, Gomez AI, Martínez CM, Angosto D, Montero MT, Herranz AS, Bazán E, Reimers D, et al. Cell volume regulation modulates NLRP3 inflammasome activation. Immunity. 2012; 37:487–500. [PubMed: 22981536]

Dahl KN, Kahn SM, Wilson KL, Discher DE. The nuclear envelope lamina network has elasticity and a compressibility limit suggestive of a molecular shock absorber. J Cell Sci. 2004; 117:4779–4786. [PubMed: 15331638]

Dahl KN, Ribeiro AJS, Lammerding J. Nuclear shape, mechanics, and mechanotransduction. Circ Res. 2008; 102:1307–1318. [PubMed: 18535268]

Davidson PM, Lammerding J. Broken nuclei - lamins, nuclear mechanics, and disease. Trends Cell Biol. 2014; 24:247–256. [PubMed: 24309562]

Enyedi B, Niethammer P. A Case for the Nuclear Membrane as a Mechanotransducer. Cell Mol Bioeng. 2016

Enyedi B, Kala S, Nikolich-Zugich T, Niethammer P. Tissue damage detection by osmotic surveillance. Nat Cell Biol. 2013; 15:1123–1130. [PubMed: 23934216]

Finan JD, Guilak F. The effects of osmotic stress on the structure and function of the cell nucleus. J Cell Biochem. 2010; 109:460–467. [PubMed: 20024954]

Friedl P, Wolf K, Lammerding J. Nuclear mechanics during cell migration. Curr Opin Cell Biol. 2011; 23:55–64. [PubMed: 21109415]

Gault WJ, Enyedi B, Niethammer P. Osmotic surveillance mediates rapid wound closure through nucleotide release. J Cell Biol. 2014; 207:767–782. [PubMed: 25533845]

Graf C, Klumpp M, Habig M, Rovina P, Billich A, Baumruker T, Oberhauser B, Bornancin F. Targeting ceramide metabolism with a potent and specific ceramide kinase inhibitor. Mol Pharmacol. 2008; 74:925–932. [PubMed: 18612076]

Guilluy C, Osborne LD, Van Landeghem L, Sharek L, Superfine R, Garcia-Mata R, Burridge K. Isolated nuclei adapt to force and reveal a mechanotransduction pathway in the nucleus. Nat Cell Biol. 2014; 16:376–381. [PubMed: 24609268]

Hamill OP, Martinac B. Molecular basis of mechanotransduction in living cells. Physiol Rev. 2001; 81:685–740. [PubMed: 11274342]

Hammond GRV, Sim Y, Lagnado L, Irvine RF. Reversible binding and rapid diffusion of proteins in complex with inositol lipids serves to coordinate free movement with spatial information. J Cell Biol. 2009; 184:297–308. [PubMed: 19153221]

Itano N, Okamoto S, Zhang D, Lipton Sa, Ruoslahti E. Cell spreading controls endoplasmic and nuclear calcium: a physical gene regulation pathway from the cell surface to the nucleus. Proc Natl Acad Sci U S A. 2003; 100:5181–5186. [PubMed: 12702768]

Izsvák Z, Chuah MKL, Vandendriessche T, Ivics Z. Efficient stable gene transfer into human cells by the Sleeping Beauty transposon vectors. Methods. 2009; 49:287–297. [PubMed: 19615447]

Kang M, Day CA, Kenworthy AK, DiBenedetto E. Simplified Equation to Extract Diffusion Coefficients from Confocal FRAP Data. Traffic. 2012; 13:1589–1600. [PubMed: 22984916]

Khatau SB, Hale CM, Stewart-Hutchinson PJ, Patel MS, Stewart CL, Searson PC, Hodzic D, Wirtz D. A perinuclear actin cap regulates nuclear shape. Proc Natl Acad Sci U S A. 2009; 106:19017–19022. [PubMed: 19850871]

Lammerding J, Schulze PC, Takahashi T, Kozlov S, Sullivan T, Kamm RD, Stewart CL, Lee RT. Lamin A/C deficiency causes defective nuclear mechanics and mechanotransduction. J Clin Invest. 2004; 113:370–378. [PubMed: 14755334]

LeBert DC, Huttenlocher A. Inflammation and wound repair. Semin Immunol. 2014; 26:315–320. [PubMed: 24853879]

Lehtonen JY, Kinnunen PK. Phospholipase A2 as a mechanosensor. Biophys J. 1995; 68:1888–1894. [PubMed: 7612831]

Liang D, Bhatta S, Gerzanich V, Simard JM. Cytotoxic edema: mechanisms of pathological cell swelling. Neurosurg Focus. 2007; 22:E2. [PubMed: 17613233]

Lichtenbergova L, Yoon ET, Cho W. Membrane penetration of cytosolic phospholipase A2 is necessary for its interfacial catalysis and arachidonate specificity. Biochemistry. 1998; 37:14128–14136. [PubMed: 9760249]

Lombardi ML, Jaalouk DE, Shanahan CM, Burke B, Roux KJ, Lammerding J. The interaction between nesprins and sun proteins at the nuclear envelope is critical for force transmission between the nucleus and cytoskeleton. J Biol Chem. 2011; 286:26743–26753. [PubMed: 21652697]

Luxton GWG, Gomes ER, Folker ES, Vintinner E, Gundersen GG. Linear arrays of nuclear envelope proteins harness retrograde actin flow for nuclear movement. Science. 2010; 329:956–959. [PubMed: 20724637]

Majno G, Joris I. Apoptosis, oncosis, and necrosis. An overview of cell death. Am J Pathol. 1995; 146:3–15. [PubMed: 7856735]

Mateus R, Pereira T, Sousa S, de Lima JE, Pascoal S, Saúde L, Jacinto A. In vivo cell and tissue dynamics underlying zebrafish fin fold regeneration. PLoS One. 2012; 7:e51766. [PubMed: 23284763]

von Moltke J, Trinidad NJ, Moayeri M, Kintzer AF, Wang SB, van Rooijen N, Brown CR, Krantz Ba, Leppla SH, Gronert K, et al. Rapid induction of inflammatory lipid mediators by the inflammasome in vivo. Nature. 2012; 490:107–111. [PubMed: 22902502]

Needham D, McIntosh TJ, Evans E. Thermomechanical and transition properties of dimyristoylphosphatidylcholine/cholesterol bilayers. Biochemistry. 1988; 27:4668–4673. [PubMed: 3167010]

Nüsslein-Volhard C, Dahm R. Zebrafish: A Practical Approach. 2002

Rock KL, Lai J-J, Kono H. Innate and adaptive immune responses to cell death. Immunol Rev. 2011; 243:191–205. [PubMed: 21884177]

Rowat AC, Lammerding J, Herrmann H, Aebi U. Towards an integrated understanding of the structure and mechanics of the cell nucleus. Bioessays. 2008; 30:226–236. [PubMed: 18293361]

Slater SJ, Kelly MB, Taddeo FJ, Ho C, Rubin E, Stubbs CD. The modulation of protein kinase C activity by membrane lipid bilayer structure. J Biol Chem. 1994; 269:4866–4871. [PubMed: 7508929]

Starr, Da; Fridolfsson, HN. Interactions between nuclei and the cytoskeleton are mediated by SUN-KASH nuclear-envelope bridges. Annu Rev Cell Dev Biol. 2010; 26:421–444. [PubMed: 20507227]

Swift J, Ivanovska IL, Buxboim a, Harada T, Dingal PCDP, Pinter J, Pajerowski JD, Spinler KR, Shin J-W, Tewari M, et al. Nuclear Lamin-A Scales with Tissue Stiffness and Enhances Matrix-Directed Differentiation. Science (80-). 2013; 341:1240104–1240104.

Thoroed SM, Lauritzen L, Lambert IH, Hansen HS, Hoffmann EK. Cell swelling activates phospholipase A2 in Ehrlich ascites tumor cells. J Membr Biol. 1997; 160:47–58. [PubMed: 9351891]

Uhlén M, Björling E, Agaton C, Szigyarto CAK, Amini B, Andersen E, Andersson AC, Angelidou P, Asplund A, Asplund C, et al. A human protein atlas for normal and cancer tissues based on antibody proteomics. Mol Cell Proteomics. 2005; 4:1920–1932. [PubMed: 16127175]

Vargas JD, Hatch EM, Anderson DJ, Hetzer MW. Transient nuclear envelope rupturing during interphase in human cancer cells. Nucleus. 3:88–100. [PubMed: 22567193]

De Vos WH, Houben F, Kamps M, Malhas A, Verheyen F, Cox J, Manders EMM, Verstraeten VLRM, van Steensel MAM, Marcelis CLM, et al. Repetitive disruptions of the nuclear envelope invoke temporary loss of cellular compartmentalization in laminopathies. Hum Mol Genet. 2011; 20:4175–4186. [PubMed: 21831885]

Vriens J, Watanabe H, Janssens a, Droogmans G, Voets T, Nilius B. Cell swelling, heat, and chemical agonists use distinct pathways for the activation of the cation channel TRPV4. Proc Natl Acad Sci U S A. 2004; 101:396–401. [PubMed: 14691263]

Watanabe H, Vriens J, Prenen J, Droogmans G, Voets T, Nilius B. Anandamide and arachidonic acid use epoxyeicosatrienoic acids to activate TRPV4 channels. Nature. 2003; 424:434–438. [PubMed: 12879072]

White RM, Sessa A, Burke C, Bowman T, LeBlanc J, Ceol C, Bourque C, Dovey M, Goessling W, Burns CE, et al. Transparent Adult Zebrafish as a Tool for In Vivo Transplantation Analysis. Cell Stem Cell. 2008; 2:183–189. [PubMed: 18371439]

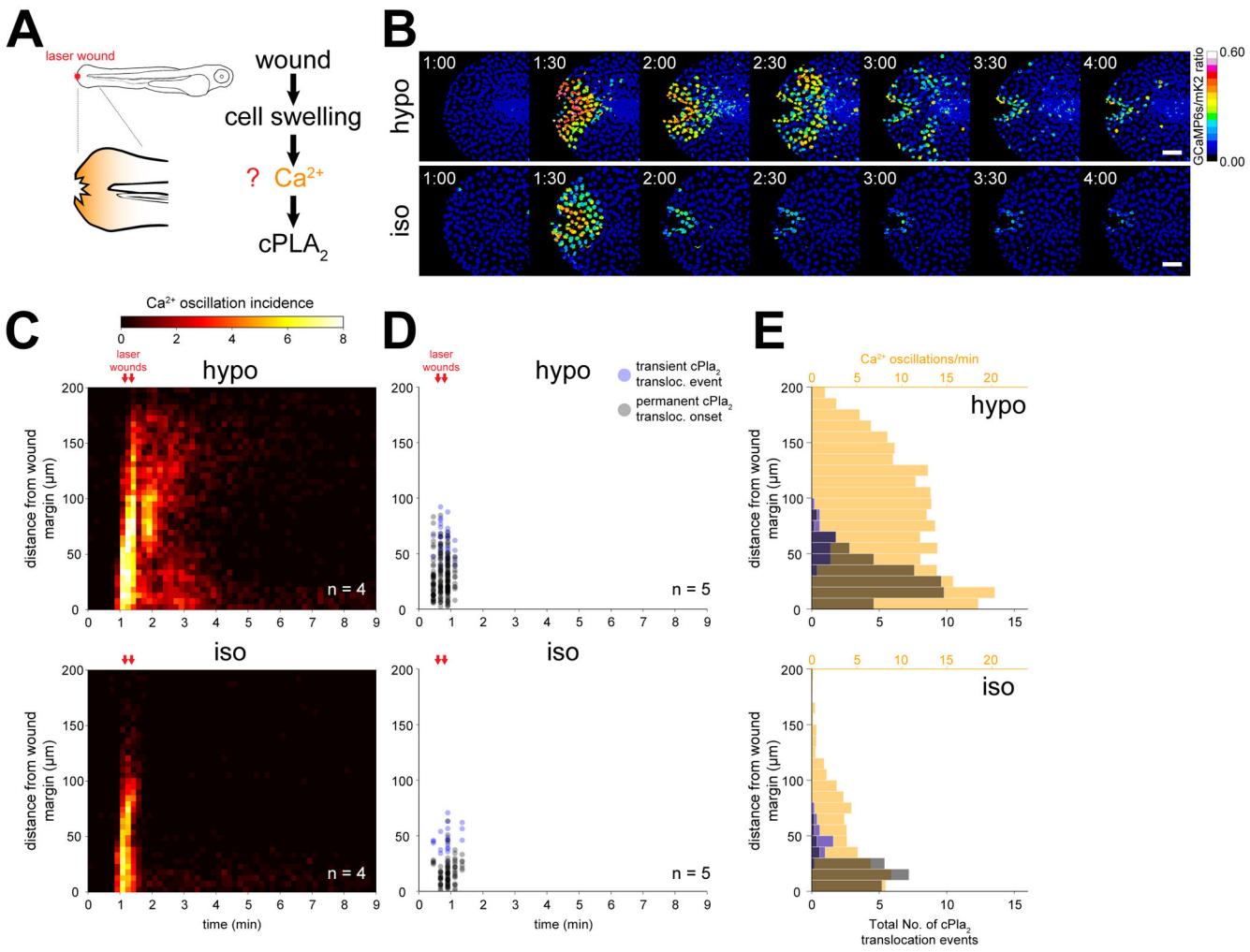

Figure 1. Osmotic shock contributes a second signal required for Ca^{2+} dependent $cPla_2$ activation in live zebrafish

(A) Left, scheme of experimental setup. Right, working hypothesis for cell swelling-induced pathway of $cPLA_2$ activation.

(B) Ratiometric imaging of Ca^{2+} transients evoked by laser-induced tail fin injury of zebrafish larvae as a function of environmental fluid osmolarity (see also Movie S1, Figure S1.). Larvae are either immersed in hypotonic solution that mimics the osmolarity of their natural habitat (“hypo”, top), or isotonic solution that mimics the osmolarity of their interstitial fluid (“iso”, bottom) to prevent cell swelling after injury. Nuclear GCaMP6s signals are normalized by nuclear mKate2 (mK2) fluorescence using the transgenic Ca^{2+} reporter larvae Tg(hsp70l:GCaMP6s-NLS-P2A-mK2-NLS). UV-laser wounding was performed at ~1 min. Scale bars, 50 µm.

(C) Averaged spatiotemporal profile of Ca^{2+} signal oscillation frequency of the indicated number of transgenic Ca^{2+} ratio-reporter larvae, wounded at the indicated times (red arrows) under hypotonic (top) or isotonic conditions (bottom).

(D) Spatiotemporal plot of permanent and transient $cPla_2$-mK2 INM-translocation events induced by wounding under hypotonic (top) and isotonic conditions (bottom) in the indicated number of Tg(hsp70l:$cPla_2$-mK2) larvae.

(E) Average spatial distribution of $cPla_2$-mK2 translocation events (blue – transient, gray – permanent) and Ca^{2+} oscillation frequency (orange) as a function of distance from the wound margin, induced by wounding larvae under hypotonic (top) or isotonic (bottom) conditions (data from experiments shown in C and D).

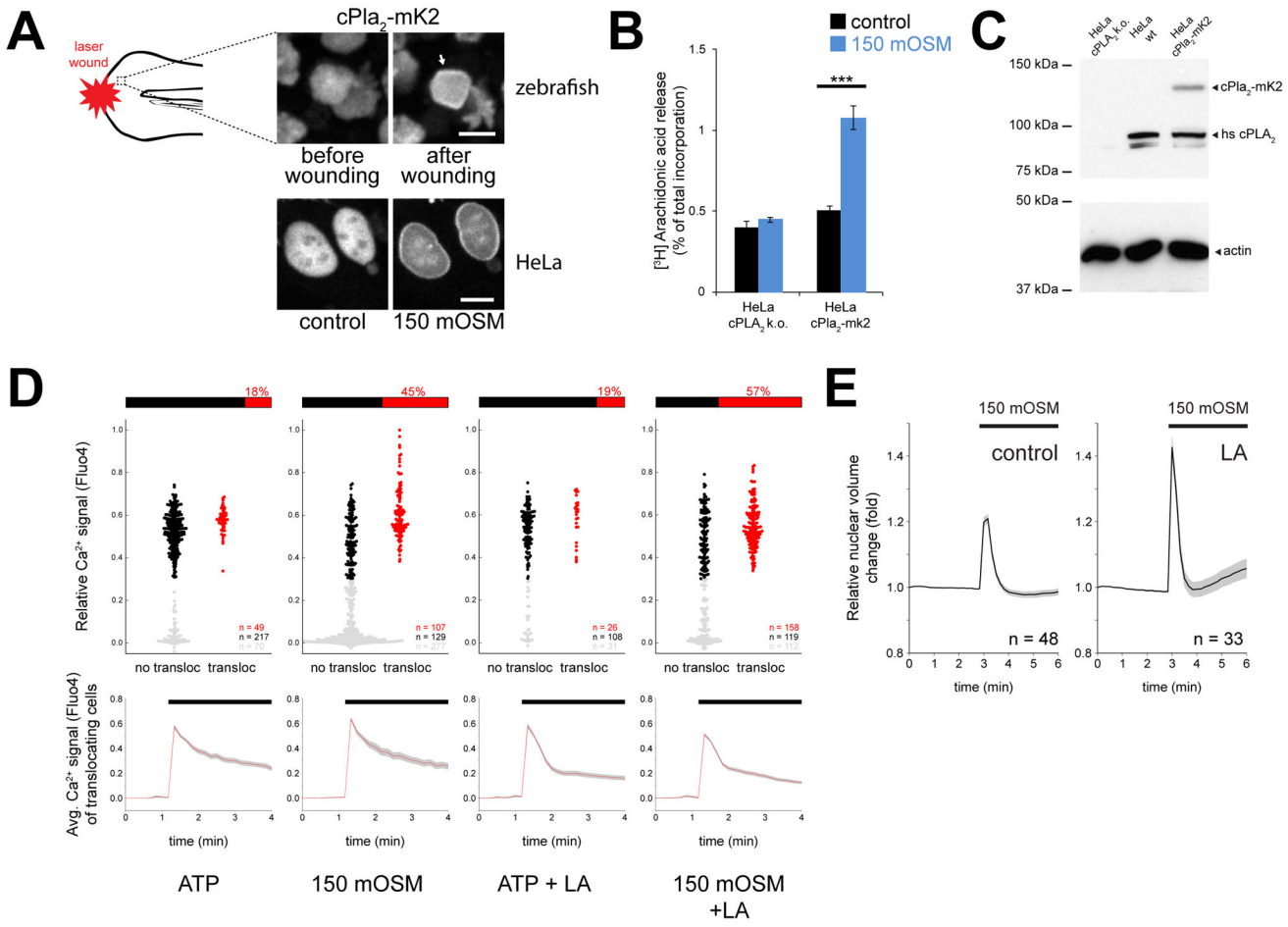

Figure 2. Osmotic shock of HeLa cells triggers cPla$_2$ translocation, AA release, and nuclear swelling counteracted by F-actin

(A) Confocal imaging of cPla$_2$-mK2 in the tail fin of larval zebrafish and HeLa cells, before and after hypotonic exposure (See also Figure S1, S3). Note the INM-accumulation of cPla$_2$ (white arrow) upon osmotic shock triggered by epithelial wounding of zebrafish in hypotonic bathing solution, or by diluting the cell culture medium of HeLa cells to 150 mOSM. Scale bars, 10 μm.

(B) [^{3}H] arachidonic acid release triggered by 10 min hypotonic shock, measured in cPLA$_2$ knock out (k.o.) HeLa cells in the absence (left bars) and presence of heterologous expression of cPla$_2$-mK2. Error bars, SEM, results from 8–10 preparations. ***, t-test $p<0.0005$.

(C) Western blot of wild type, cPLA$_2$ knock out, and cPla$_2$-mK2-expressing HeLa cells.

(D) Parallel, single cell measurements of cPla$_2$-mK2 INM-translocation and cytoplasmic Ca^{2+} signals, using the calcium indicator dye Fluo4. INM-translocation and Fluo4 signals were scored by automated image analysis. Fluo4 signals were normalized to baseline values and ionomycin-induced maximum signals (see Methods for details). Upper panels, plot of cPla$_2$-mk2 translocation (x-axis) as a function [Ca^{2+}] (y-axis) in the same cell. Cellular responses were triggered by the purinergic agonist ATP (100 μM) or hypotonicity (150 mOSM) in the absence/presence of latrunculin A (LA) pretreatment as indicated. Gray dots,

cells with Ca^{2+} signals below the critical threshold required for $cPla_2$-mK2 translocation. Black dots, cells above the critical Ca^{2+}-threshold (i.e., 0.3) that do not show $cPla_2$-mK2 translocation. Red dots, cells above the critical Ca^{2+}-threshold showing $cPla_2$-mK2 translocation. The percentage of translocating (red) versus non-translocating cells (black) above the critical Ca^{2+}-threshold is depicted as bar diagram above each plot. This ratio indicates the efficiency of a suprathreshold Ca^{2+} signal to induce $cPla_2$-mK2 translocation under the respective experimental condition. Lower panels, average $[Ca^{2+}]$-traces of cells that exhibit $cPla_2$-mK2 translocation during the stimulation. Error bars, SEM. n, number of cells.

(E) Average nuclear volume evolution after hypotonic shock in untreated and LA-pretreated HeLa cells, measured by confocal imaging of nuclear targeted EGFP. Error bars, SEM. n, number of cells.

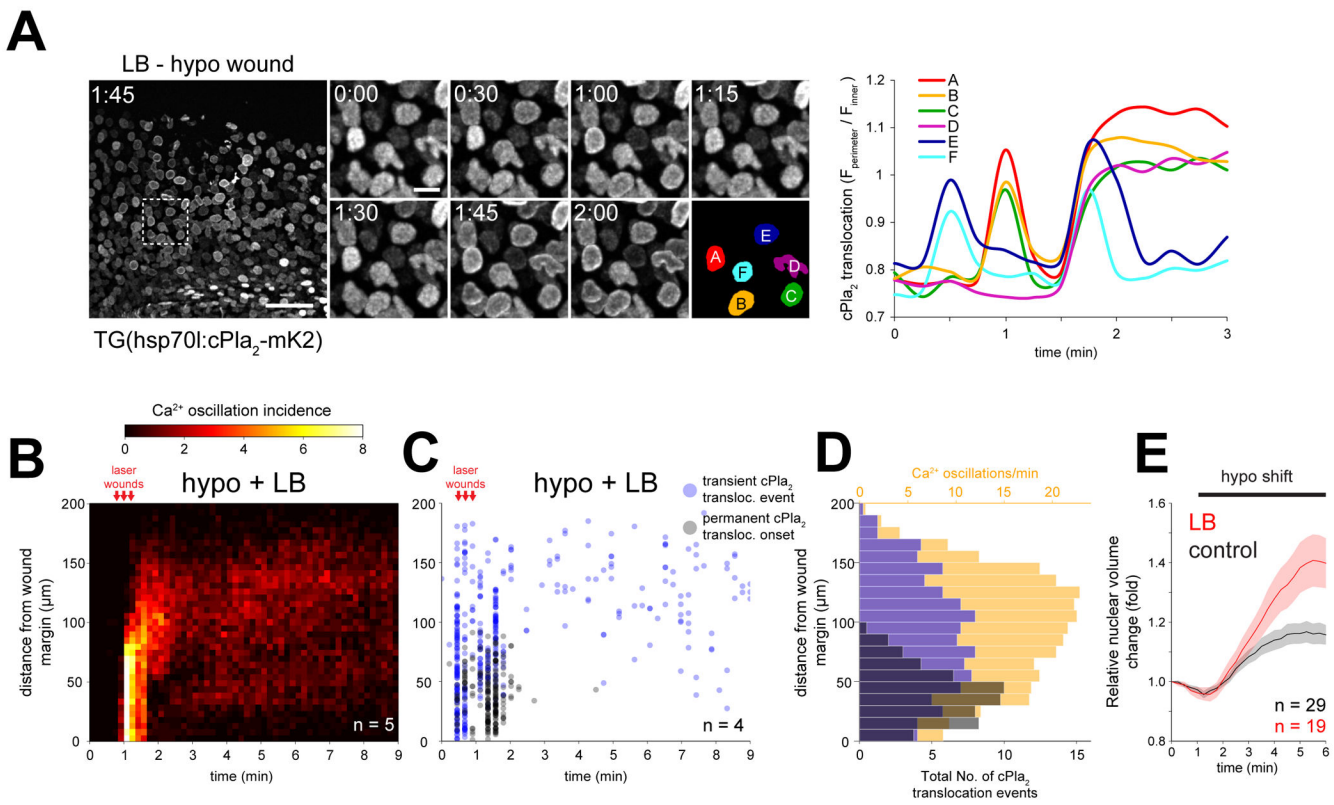

Figure 3. F-actin inhibits cPla$_2$ translocation and nuclear swelling in live zebrafish

(A) Left panel, confocal maximum intensity projections of cPla$_2$-mK2 in latrunculin B (LB) pretreated zebrafish larvae, wounded under hypotonic conditions at t=0.5–1 min. Note the wave of cPla$_2$-mK2 translocation reaching ~200 µm deep into the tissue (also see Movie S4). Scale bars, 50 and 10 µm. Right panel, quantification of cPla$_2$-mK2 translocation (see Methods for details) in selected nuclei, marked with rainbow color masks (A–F) on the left panel.

(B) Averaged spatiotemporal profile of Ca^{2+} signal oscillation frequency of the indicated number of transgenic Ca^{2+} ratio-reporter larvae, pretreated with latrunculin B (LB) and wounded at the indicated time under hypotonic conditions.

(C) Spatiotemporal plot of permanent and transient cPla$_2$-mK2 INM-translocation events induced by wounding under hypotonic conditions after LB-pretreatment in the indicated number of Tg(hsp70l:cPla$_2$-mK2) larvae.

(D) Average spatial distribution of cPla$_2$-mK2 translocation events (blue – transient, gray – permanent) and Ca^{2+} oscillation frequency (orange) as a function of distance from the wound margin, induced by wounding LB-pretreated larvae under hypotonic conditions (data from experiments shown in B and C).

(E) Average nuclear volume evolution in the suprabasal and basal epithelial cells of zebrafish tail fin after hypotonic shifting in untreated and LB-pretreated larvae, measured by confocal imaging of nuclear targeted EGFP. Error bars, SEM. n, number of cells.

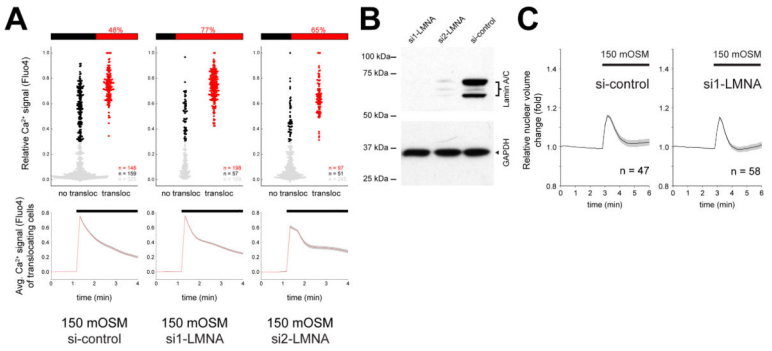

Figure 4. Lamin A/C inhibits cPla$_2$ translocation after osmotic shock of HeLa cells

(A) Parallel measurements of cytoplasmic Ca^{2+} signals and cPla$_2$-mK2 translocation to the nuclear membrane in control (si-control) and LMNA knockdown HeLa cells (si1-LMNA and si2-LMNA). Ca^{2+} signals were stimulated by hypotonic swelling (150 mOSM), and the efficiency of Ca^{2+} signals to induce cPla$_2$-mK2 translocation was assessed. The data representation is analogous to Fig. 2D and is explained there. n, number of cells.

(B) Western blot of Lamin A/C knockdown (si1-LMNA and si2-LMNA) and control siRNA treated HeLa cells.

(C) Average nuclear volume evolution after hypotonic shock in Lamin A/C knockdown (si1-LMNA) and control siRNA treated HeLa cells, measured by confocal imaging of nuclear targeted EGFP. Error bars, SEM. n, number of cells.

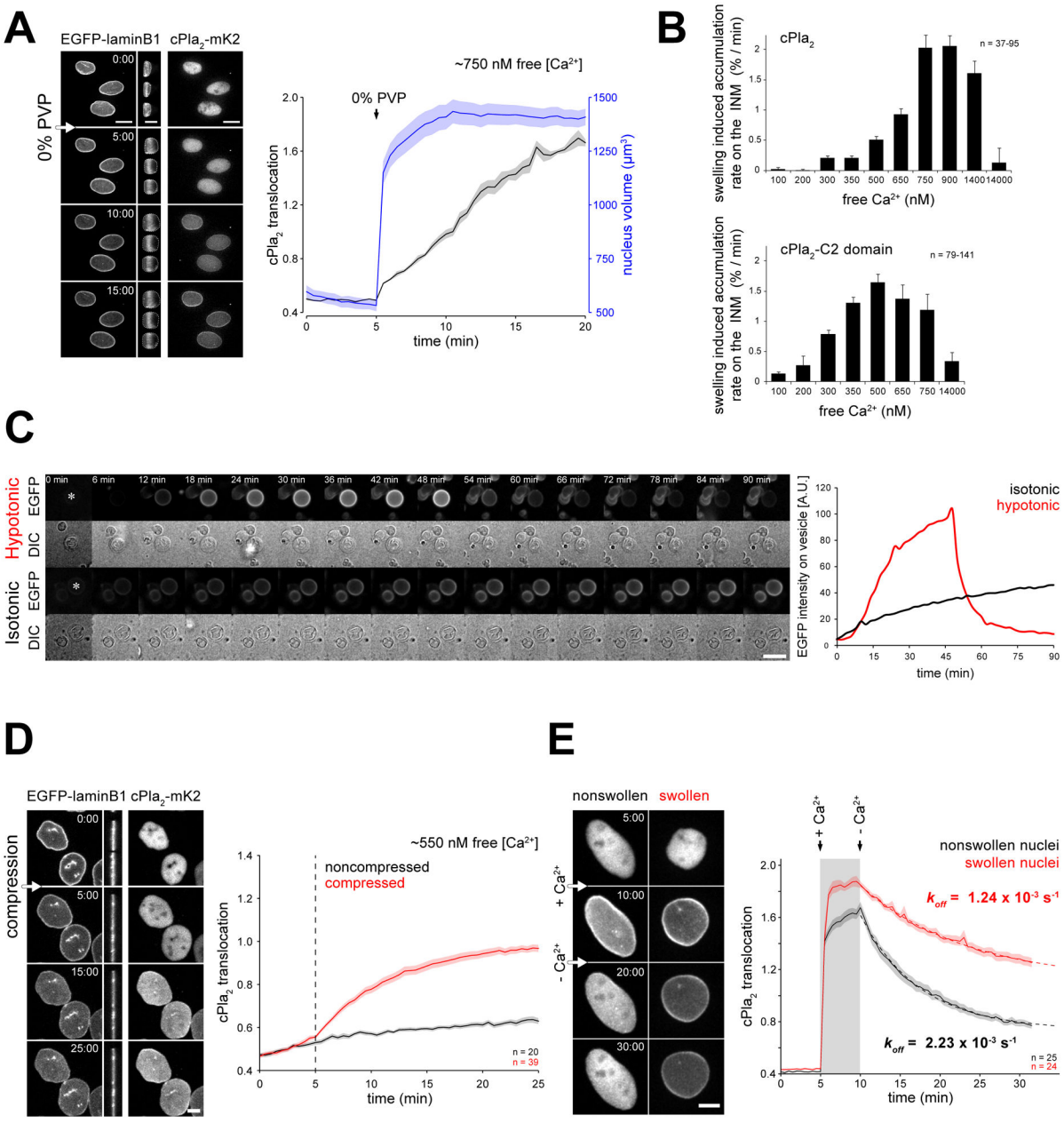

Figure 5. Nuclear swelling or compression promotes cPla$_2$ accumulation on the INM

(A) Left panel, confocal images of cPla$_2$-mK2 and EGFP-laminB1 fluorescence in permeabilized HeLa cells. Cells were treated with digitonin for 10 min before imaging in medium containing ~750 nM free [Ca^{2+}] and 2.5% PVP. Note the nuclear swelling induced by PVP-washout at t = 5 min, visible on the side-view projections and quantified on the right (outlines of nuclei are marked by dashed white line). Right panel, average plot of nuclear volume and cPla$_2$-mK2 translocation of the depicted nuclei. Note that swelling coincides with the onset of cPla$_2$-mk2 accumulation on the nuclear envelope (also see Movie S5).

(B) Rate of $cPla_2$ (top) and $cPla_2$-C2-domain (bottom) accumulation on the nuclear membrane in response to nuclear swelling at different free Ca^{2+} concentrations (see Methods for details and Figure S4, S5). Error bars, SEM. n, number of cells.
(C) Left panel, representative time-lapse montage of GVs filled with PBS + 300 mM Sucrose immersed in PBS (hypotonic- relative to GV interior) or PBS + 300 mM Sucrose (isotonic) in the presence of 0.5 mM $CaCl_2$ and 9.3 μM recombinant $cPla_2$-C2-EGFP (also see Movie S6). Scale bar, 20 μm. Right panel, average EGFP intensity measured in a 5x5 μm square center region of the vesicles indicated by a white asterisk in the first frame.
(D) Representative confocal images and quantification of $cPla_2$-mK2 accumulation on the nuclear membrane after mechanical compression (also see Movie S7). Cells were permeabilized with digitonin for 5 min before imaging in medium containing ~550 nM free [Ca^{2+}] and 2.5% PVP. The nuclei were then compressed (red) or left untreated (black). Note the nuclear compression at t = 5 min, visible on the side-view projections of the EGFP-laminB1 fluorescence images. Error bars, SEM. n, number of cells.
(E) Representative confocal images and quantification of $cPla_2$-mK2 dissociation from the nuclear membrane after Ca^{2+}-washout (also see Movie S8). Cells were first permeabilized in intracellular medium containing 2.5% PVP at low free [Ca^{2+}] (0.1 μM). Then, the supernatant was swapped to medium with high free [Ca^{2+}] (14 μM) with or without PVP to allow the nuclei to maintain their size or swell, respectively. After 5 min, when $cPla_2$-mK2 was fully translocated to the INM, cells were washed with low [Ca^{2+}] medium with or without PVP, which initiated $cPLA_2$ dissociation from the nonswollen and swollen nuclei. The apparent k_{off} of $cPla_2$-mK2, indicating membrane debinding, was calculated from an exponential fit (dashed line). Scale bars, 10 μm. Error bars, SEM. n, number of cells.

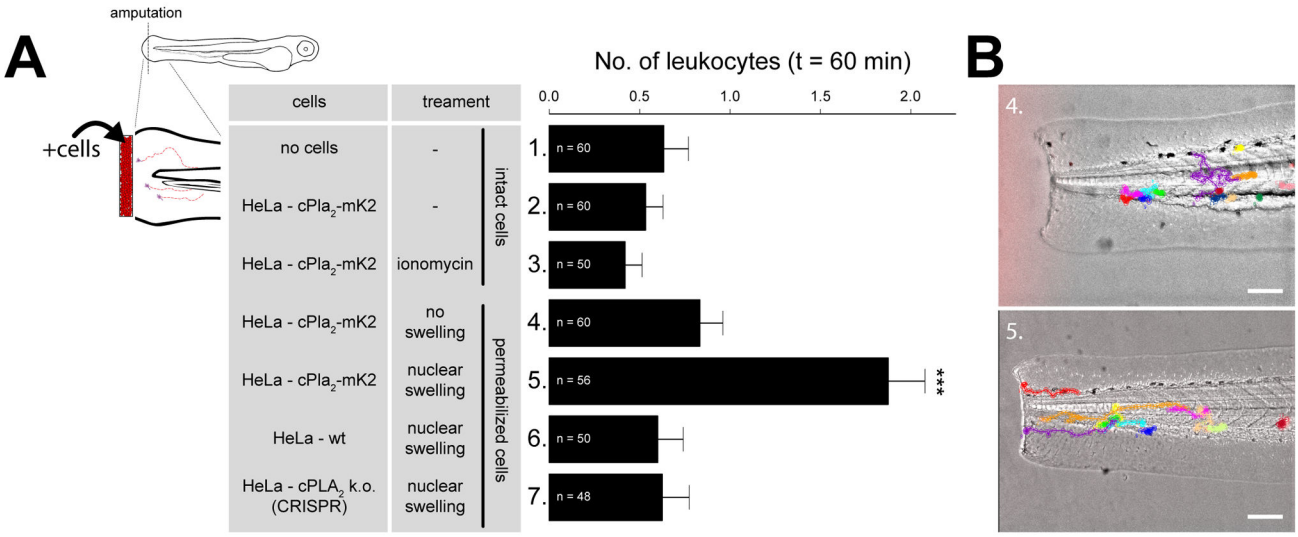

Figure 6. Swollen nuclei that contain cPla$_2$ attract leukocytes to cell corpses

(A) Left panel, scheme of experimental design. Amputated zebrafish larvae were immersed in isotonic bathing solution to inhibit endogenous, wound-induced inflammation. Amputation wounds were exposed to differently conditioned HeLa cell suspensions. Nuclear swelling was initiated by digitonin-permeabilization and blocked by PVP-supplementation as described. Right panel, average number of leukocytes recruited to the wound margin within 60 min after cell-exposure of amputated tail fins at indicated conditions (table). Note that only swollen (condition #5), but not nonswollen nuclei (condition #3 and #4) that contain cPla$_2$-mK2 attract leukocytes to cell corpses at permissive [Ca^{2+}]. Error bars, SEM. ***, t-test $p<0.0005$. n, number of animals.

(B) Transmitted light images of zebrafish larvae exposed to permeabilized cell corpses with non-swollen (top, condition #4) or swollen (bottom, condition #5) nuclei that contain cPla$_2$-mK2. Representative leukocyte tracks are superimposed and color-coded. Please refer to Methods for details. Scale bars, 100 μm.

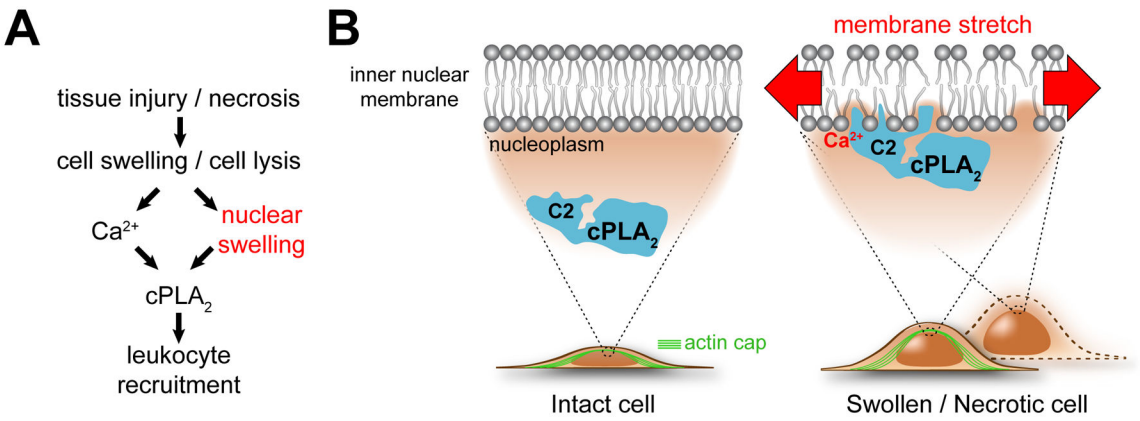

Figure 7. Proposed regulatory scheme

(A) Simplified pathway diagram. Pathological tissue perturbations such as wounding, ischemia or blunt trauma cause cell swelling and lysis. Both events trigger nuclear swelling. Nuclear swelling is an important second signal, besides Ca^{2+}, for $cPla_2$-dependent leukocyte recruitment.

(B) Hypothetical mechanosensing scheme. Nuclear swelling, probably through stretch-induced changes in lipid packing, facilitates hydrophobic insertion of the enzyme into the bilayer core (via its C2-domain), which is required for its activity. In intact cells, nuclear swelling is initiated by cell swelling and restricted by a nuclear actin cap, and maybe other F-actin structures (for example, cortex, TAN lines (Luxton et al., 2010), etc.). In permeabilized cells, actin filaments are gone and nuclei completely expand in response to loss of cytoplasmic macromolecules. Like the nuclear lamina, F-actin probably contributes to nuclear envelope stabilization, dampening forces that act on the nuclear membrane. Thereby it counteracts swelling-induced $cPla_2$ activation.